

Human face rendering

A document for works done so far

Shengze Zhang

Digital Art Laboratory, Shanghai Jiao Tong University

References and links

- [1] Krishnaswamy, Aravind. "BioSpec: A biophysically-based spectral model of light interaction with human skin." (2005).
- [2] Jensen, Henrik Wann, et al. "A practical model for subsurface light transport." *Proceedings of the 28th annual conference on Computer graphics and interactive techniques*. ACM, 2001.
- [3] Donner, Craig, and Henrik Wann Jensen. "A spectral BSSRDF for shading human skin." *Proceedings of the 17th Eurographics conference on Rendering Techniques*. Eurographics Association, 2006.
- [4] Meglinski, I. V., and S. J. Matcher. "Computer simulation of the skin reflectance spectra." *Computer Methods and Programs in Biomedicine* 70.2 (2003): 179-186.
- [5] Petrov, Georgi I., et al. "Human tissue color as viewed in high dynamic range optical spectral transmission measurements." *Biomedical optics express* 3.9 (2012): 2154.
- [6] Tsumura, Norimichi, et al. "Image-based skin color and texture analysis/synthesis by extracting hemoglobin and melanin information in the skin." *ACM Transactions on Graphics (TOG)*. Vol. 22. No. 3. ACM, 2003.
- [7] Saidi, Iyad S., Steven L. Jacques, and Frank K. Tittel. "Mie and Rayleigh modeling of visible-light scattering in neonatal skin." *Applied optics* 34.31 (1995): 7410-7418.
- [8] Wang, Lihong, and Steven L. Jacques. "Monte Carlo modeling of light transport in multi-layered tissues in standard C." *The University of Texas, MD Anderson Cancer Center, Houston* (1992).
- [9] Ghosh, Abhijeet, et al. "Practical modeling and acquisition of layered facial reflectance." *ACM Transactions on Graphics (TOG)* 27.5 (2008): 139.
- [10] Li, Ling, and Carmen So-Ling Ng. "Rendering human skin using a multilayer reflection model." *Int J Math Comput Simulat* 3.1 (2009): 44-53.
- [11] Igarashi, Takanori, Ko Nishino, and Shree K. Nayar. "The appearance of human skin." (2005).
- [12] Jacques, S. "Skin optics summary." *Oregon Medical Laser Center News*(1998). <http://omlc.ogi.edu/news/jan98/skinoptics.html>.
- [13] Prah, Scott. "Optical absorption of hemoglobin." (1999). <http://omlc.ogi.edu/spectra/hemoglobin/index.html>

- [14]2-deg XYZ CMFs transformed from the CIE (2006) 2-deg LMS cone fundamentals. <http://cvrl.ioo.ucl.ac.uk/cmfs.htm>
- [15]CIE 1931 color space.
http://en.wikipedia.org/wiki/CIE_1931_color_space
- [16]sRGB. <http://en.wikipedia.org/wiki/SRGB>
- [17]Monte Carlo method for photon transport.
http://en.wikipedia.org/wiki/Monte_Carlo_method_for_photon_transport#Biomedical_applications_of_Monte_Carlo_methods
- [18]Van Gemert, M. J. C., et al. "Skin optics." *Biomedical Engineering, IEEE Transactions on* 36.12 (1989): 1146-1154.
- [19]Bashkatov, A. N., et al. "Optical properties of human skin, subcutaneous and mucous tissues in the wavelength range from 400 to 2000 nm." *Journal of Physics D: Applied Physics* 38.15 (2005): 2543.
- [20]Beer-Lambert Law.
http://en.wikipedia.org/wiki/Beer%E2%80%93Lambert_law
- [21]Zhu, Caigang, and Quan Liu. "Review of Monte Carlo modeling of light transport in tissues." *Journal of biomedical optics* 18.5 (2013): 050902-050902.

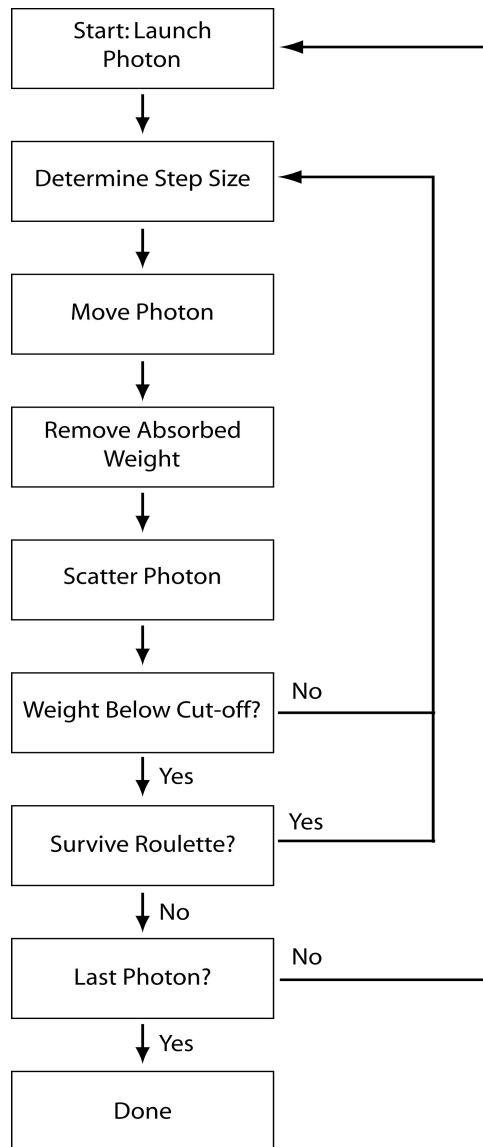
1. A brief introduction

Several different methods are applied in human face rendering. A image-based practical method for modeling layered facial reflectance is applied in rendering human face[9], other image-based texture analysis and synthesis is also applied to determine the skin color[6]. Jensen introduces a practical model for subsurface light transport[2] and a spectral-dependent practical BSSRDF model for shading human skin[3]. Monte Carlo methods is also applied in determining human skin color and modeling human skin reflectance[1,4-5,10].

Our work is mainly based on Monte Carlo ray tracing method[8] to simulate real photon transfer in human skin tissue, by which to determine the human skin color.

2. Method and model

MC ray tracing method is implemented by MC modeling of light transport in multilayered tissues constructed by L. Wang[8]. A simple workflow is showed below[17].



parameters:

§: random number in range(0,1)

t: interaction coefficient, sum of absorption coefficient and scattering coefficient

a: absorption coefficient

s: reduced scattering coefficient

x,y,z: position

dx,dy,dz: direction

w: weight

θ: scattering deflection angle

Ψ: scattering azimuthal angle

g: scattering anisotropy

step 1: launch a photon packet, and initial it's weight, position and direction

step 2: determine the step size of this step

$$s = -\ln \xi / t$$

Then move the photon.

$$x = x + dx * s$$

$$y = y + dy * s$$

$$z = z + dz * s$$

step 3: absorption.

$$w = w - a/t * w$$

scattering.

$$\cos \theta = \begin{cases} \frac{1}{2g} \left[1 + g^2 - \left(\frac{1-g^2}{1-g+2g\xi} \right)^2 \right] & \text{if } g \neq 0 \\ 1 - 2\xi & \text{if } g = 0 \end{cases}$$

$$\varphi = 2\pi\xi$$

$$\mu'_x = \frac{\sin \theta (\mu_x \mu_z \cos \varphi - \mu_y \sin \varphi)}{\sqrt{1 - \mu_z^2}} + \mu_x \cos \theta$$

$$\mu'_y = \frac{\sin \theta (\mu_y \mu_z \cos \varphi + \mu_x \sin \varphi)}{\sqrt{1 - \mu_z^2}} + \mu_y \cos \theta$$

$$\mu'_z = -\sqrt{1 - \mu_z^2} \sin \theta \cos \varphi + \mu_z \cos \theta$$

for dz = -+1

$$\mu'_x = \sin \theta \cos \Psi$$

$$\mu'_y = \sin \theta \sin \Psi$$

$$\mu'_z = \text{SIGN}(\mu_z) \cos \theta$$

step 4: termination, a roulette technique is employed for photon weight below a threshold (for example 0.0001, m = 10)

$$W = \begin{cases} mW & \xi \leq 1/m \\ 0 & \xi > 1/m \end{cases}$$

step 5: hitting boundary.

Internal reflection or escape from boundary based on the Fresnel's formulas and Snell's law.

$$R(\alpha_i) = \frac{1}{2} \left[\frac{\sin^2(a_i - a_t)}{\sin^2(a_i + a_t)} + \frac{\tan^2(a_i - a_t)}{\tan^2(a_i + a_t)} \right]$$

If $\xi \leq R(a_i)$, then photon is internally reflected;

If $\xi > R(a_i)$, then photon escapes the tissue.

Besides the MC method, the parameter model is another important part of the simulation of photon transport, including anisotropy, scattering coefficient, dermis absorption coefficient, epidermis absorption coefficient[1,7-8,12-13,18].

Gemert *et al.* have proposed an empirical equation that relates the anisotropy factor g to the wavelength[18].

Anisotropy factors of both the epidermis and the dermis are given by

$$g = 0.62 + 0.29 * 10^{-3} * \lambda$$

Reduced scattering coefficient of the epidermis and the dermis are approximated the same, for that the scattering in epidermis is negligible due to its thin thickness. Scattering coefficient is based on the combination of Mie scattering and Rayleigh scattering[7,12,19], but the approximation of two scattering is partly different from article to article.

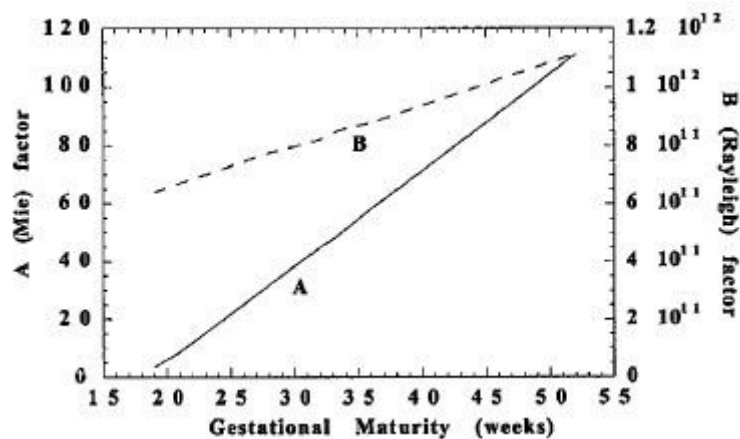
The approximation equation proposed by Jacque[12] is

$$s = 2 * 10^4 * \lambda^{-1.5} + 2 * 10^{11} * \lambda^{-4}$$

Reduced scattering coefficient is measured by Saidi et al. are fitted through the equation[7]

$$s = A * [1 - (1.745 * 10^{-3}) * \lambda + (9.843 * 10^{-7}) * \lambda^2] + B * \lambda^{-4}$$

The determined values of the fitting parameters A and B are plotted in figure below as a function of gestational age.



(Noting: the value of the A and B plotted in the function is for reduced scattering coefficient in cm⁻¹, all of the other coefficients in this document is mm⁻¹)

The value of A and B of skin with typical 36-week gestational maturity is approximately 57 and 8.4 * 10¹¹. So the reduced scattering coefficient can be fitted

through the equation

$$s = 5.7*[1-(1.745*10^{-3})*\lambda+(9.843*10^{-7})*\lambda^2] + 8.4*10^{10}*\lambda^{-4} \text{ (mm-1)}$$

Bashkatov et al. also measure the reduced scattering coefficient and fit it through an approximation equation[19]

$$s = 7.37*\lambda^{-0.22} + 1.1*10^{11}*\lambda^{-4}$$

However, what is confusing is that in two articles[3,5], authors propose the approximation of the reduced scattering coefficient in the equation below,

$$s = 14.74*\lambda^{-0.22} + 2.2*10^{11}*\lambda^{-4} \text{ (used in our model),}$$

and one of them is cited from Bashkatov's paper[19] and the other is cited from Saidi's paper[7].

The equation just above is used in our algorithm.

Epidermis absorption coefficient is calculated by

$$a_{\text{epi}} = (f_{\text{mel}})(a_{\text{mel}}) + (1 - f_{\text{mel}})(a_{\text{skinbase}})[12],$$

in which f_{mel} is the fraction of melanin and a_{mel} and a_{skinbase} is the absorption coefficient of melanin and skinbase.

$$a_{\text{mel}} = f_{\text{emel}} * a_{\text{emel}} + (1 - f_{\text{emel}}) * a_{\text{pmel}}[3],$$

in which f_{emel} is the proportion of eumelanin in melanin and $1 - f_{\text{emel}}$ is the proportion of pheomelanin in melanin.

$$a_{\text{emel}} = 6.6*10^{10}*\lambda^{-3.33}$$

$$a_{\text{pmel}} = 2.9*10^{14}*\lambda^{-4.75}$$

$$a_{\text{skinbase}} = 0.0244 + 8.53\exp(-(\lambda - 154)/66.2)$$

Dermis absorption coefficient is calculated by

$$a_{\text{der}} = (f_{\text{h}})(a_{\text{h}}) + (1 - f_{\text{h}})(a_{\text{skinbase}})[12],$$

in which f_{h} is the fraction of hemoglobin and a_{h} is the absorption coefficient of hemoglobin.

$$a_{\text{h}} = f_{\text{oxyh}} * a_{\text{oxyh}} + (1-f_{\text{oxyh}}) * a_{\text{deoxyh}}[3],$$

in which f_{oxyh} is the proportion of oxy-hemoglobin in hemoglobin and $1 - f_{\text{oxyh}}$ is the proportion of deoxy-hemoglobin in hemoglobin.

f_{oxyh} is fixed in 0.7 in our model and data of a_{oxyh} and a_{deoxyh} can be obtained online[13].

3. Different computing models of absorption

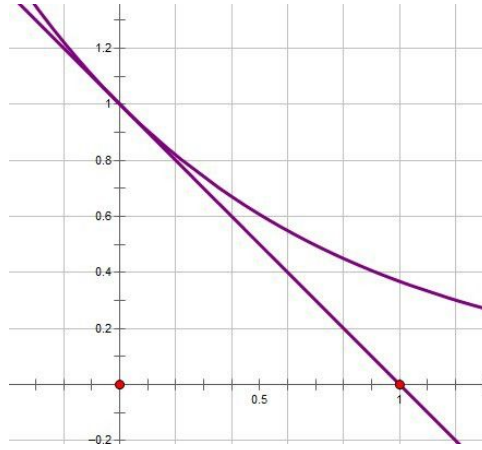
The computing model of absorption mentioned above is described by L. Wang[8]. However, the basic principle of absorption is Beer-Lambert's law, which is not a linear decrease but an exponential decrease instead[20].

$$s = -\ln\$/t, \text{ which averages in } 1/t, \text{ for the average of } -\ln\$/ \text{ is equal to } 1.$$

$w = (1 - a/t)*w$, in average $1/t = s$, so the equation $w = (1 - a * s)w$ can be obtained, a linear decrease.

For the standard Beer-Lambert's law, the absorption equation should be $w = e^{-(a * s)w}$.

The decrease terms differ in $1 - x$ and e^{-x} . The plane coordinate curves are showed in the figure below.



A slight difference occurs when x is very small and the difference increase as x increase, so the difference that influences the final simulation color of human skin become larger when the absorption coefficient is larger. A comparison of two methods is given in the result section.

The linear absorption is a good approximation when absorption coefficient is relatively small and a sound alternative for exponential computing model when faster computation speed is needed, for the exponential operation is much lower in speed than linear plus and minus operation.

4. BSSRDF

The direction of a ray hitting a 3-D mesh of the model is firstly convert into a normal-binormal-tangent based coordinate system by a 4*4 matrix. Then the propagation in the skin tissue is simulated in the normalized coordinate system. Besides the output weight, recorded as reflectance of skin, the outgoing point is calculated. After converting the out point back into the world coordinate system, the point will be projected into the real out point on 3-D mesh of the model for further calculation. Thus the outgoing point is significantly different from the incoming point, in other words fulfilling the BSSRDF model.

5. sRGB

Whatever simulating skin color only or rendering the 3-D mesh, we will get a relative reflectance spectral power distribution of the human skin in the specific parameter setting, which determines the skin color. The algorithm for converting the spectral power distribution into sRGB model, which can be displayed in a computer display device, is given below[15,16].

step1: From relative reflectance SPD $I(\lambda)$ to CIE XYZ color space

$$X = \int_{380}^{780} I(\lambda) \bar{x}(\lambda) d\lambda$$

$$Y = \int_{380}^{780} I(\lambda) \bar{y}(\lambda) d\lambda$$

$$Z = \int_{380}^{780} I(\lambda) \bar{z}(\lambda) d\lambda$$

$\bar{x}(\lambda)$ is the CIE's color matching function of X, which can be obtained online.

step2: Normalization and setting white point.

The white point of XYZ space is based on a constant SPD, in other word (1,1,1) for XYZ value after normalization. However, the white point of sRGB model is D65, the value of which in XYZ model is (0.9505, 1, 1.089). Therefore, a normalization to unity and scaling each value of XYZ to D65 white point is needed.

step3: From XYZ color space to intermediate linear parameters

$$\begin{bmatrix} R_{\text{linear}} \\ G_{\text{linear}} \\ B_{\text{linear}} \end{bmatrix} = \begin{bmatrix} 3.2406 & -1.5372 & -0.4986 \\ -0.9689 & 1.8758 & 0.0415 \\ 0.0557 & -0.2040 & 1.0570 \end{bmatrix} \begin{bmatrix} X \\ Y \\ Z \end{bmatrix}$$

$(R_l, G_l, B_l) = (1,1,1)$ when $(X, Y, Z) = (0.9505, 1, 1.089)$

Each value of the intermediate linear parameters can be out of range(0,1), so a clipping is needed.

step4: Correcting gamma value to 2.2, converting into sRGB model.

sRGB was designed to reflect a typical real-world monitor with a gamma of 2.2, and the following formula transforms the linear values into sRGB.

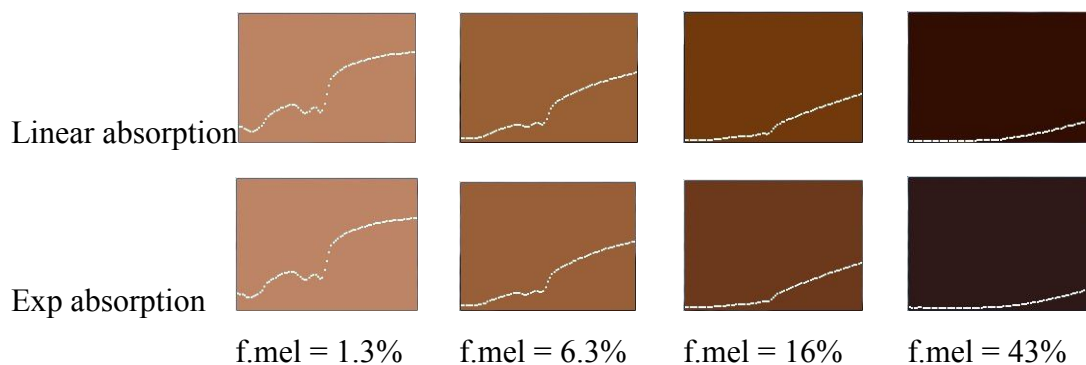
$$C_{\text{srgb}} = \begin{cases} 12.92C_{\text{linear}}, & C_{\text{linear}} \leq 0.0031308 \\ (1 + a)C_{\text{linear}}^{1/2.4} - a, & C_{\text{linear}} > 0.0031308 \end{cases}$$

$a = 0.055$.

These values can be set to data array for final displaying on the device.

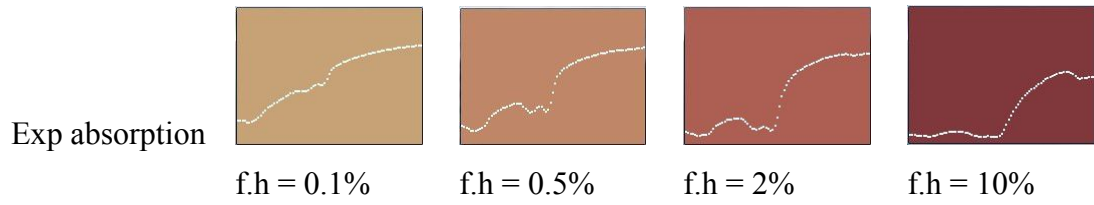
6. Result and limitation

Change in skin color as melanin volume fraction f_{mel} from 1.3% to 43%. The eumelanin fraction is fixed at 0.7, hemoglobin fraction is fixed at 0.5%.

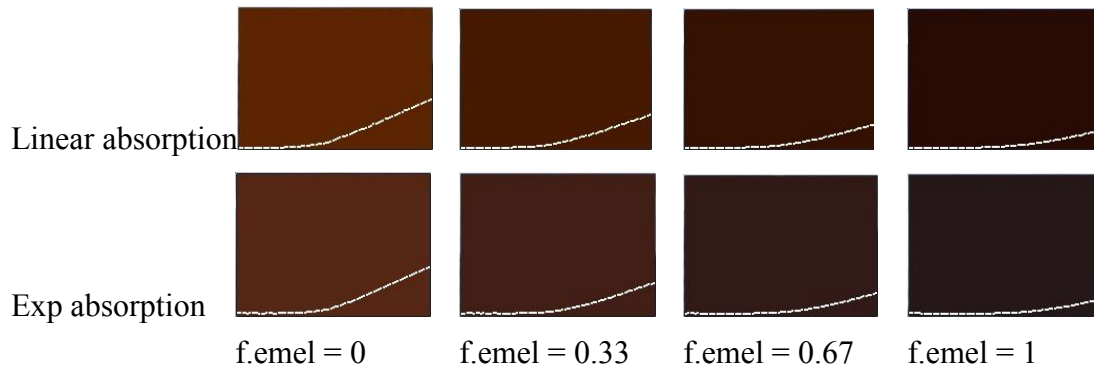


Change in skin color as hemoglobin fraction f_{h} from 0.1% to 10%. The melanin fraction is fixed at 1.3%, with eumelanin fraction at 0.5.

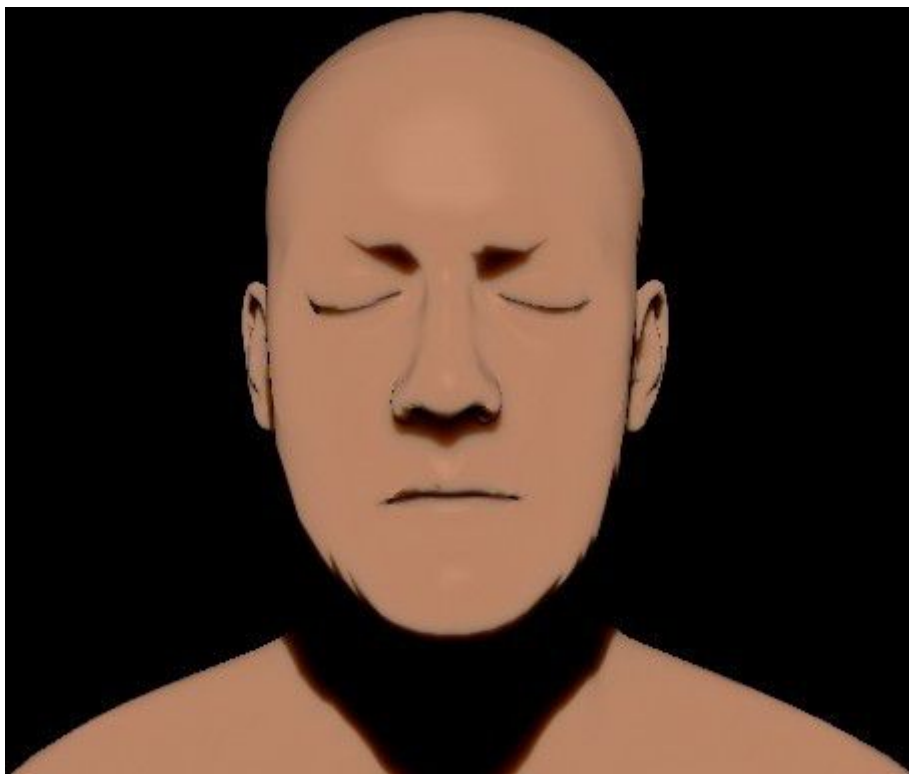




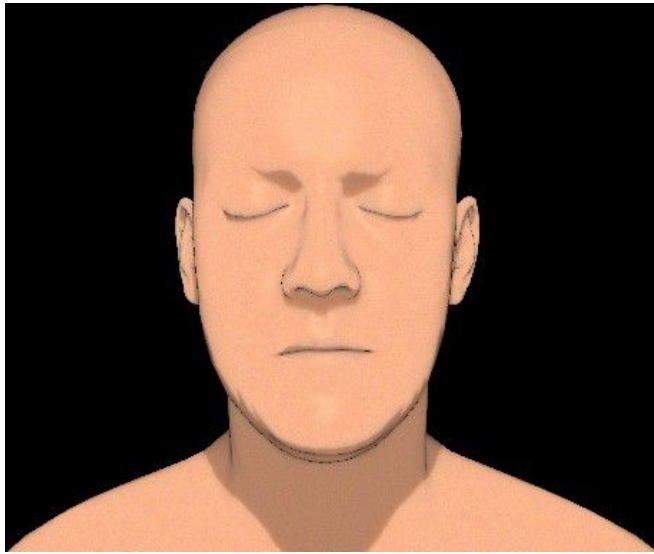
Change in skin color as eumelanin fraction $f.emel$ from 0 to 1. The melanin fraction is fixed at 43%. The hemoglobin fraction is constant at 0.1%.



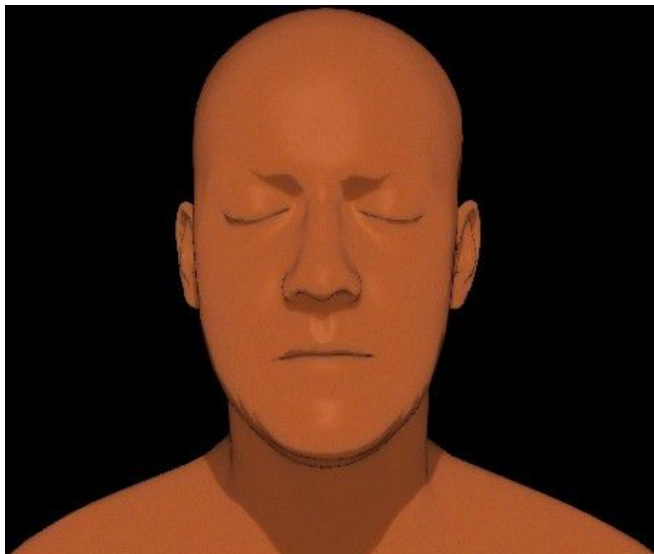
A 3-D mesh model rendered by BSSRDF model mentioned is showed in the figure below. The 500-sample result needs more than 10 hours to rendering.



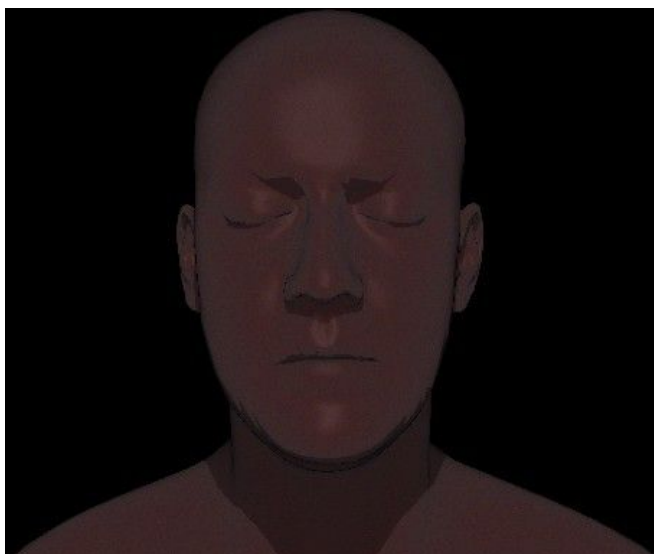
Different skin types are simulated with our model. For Caucasian skin, $f.m = 1.3\%$, $f.em = 0.7$ and $f.h = 0.5\%$. For Asian skin, $f.m = 16\%$, $f.em = 0$ and $f.h = 1\%$. For African skin, $f.m = 43\%$, $f.em = 0.7$ and $f.h = 1\%$.



Caucasian,20-sample



Asian,55-sample



African,150-sample

Compared to works done by Petrox et al. [5] and C. Donner and H.W. Jensen [3], the skin colors in the similar coefficient setting are different more or less.

Besides, the biggest limitation in our work is the lack of real skin rendering instead of single skin color and the lack of texturing, such as local color variation (lip) and face details (pores, wrinkles) in rendering 3-D mesh [2-3,5].

Another limitation is the propagation in the skin tissue, during which an assumption that skin is semi-infinite is made, which may be a significant error in mesh position with low radius (nose, ears etc.). To overcome this limitation, a propagation algorithm taking real mesh geometry into account is needed, instead of converting into standard coordinate before propagation.

At last, a relative low computing speed is another major limitation for a 500-sample 3-D mesh rendering needs at least 10 hours to complete. Additional speed-up optimization is needed in the future work [21].